

This work was written as part of one of the author's official duties as an Employee of the United States Government and is therefore a work of the United States Government. In accordance with 17 U.S.C. 105, no copyright protection is available for such works under U.S. Law.

Public Domain Mark 1.0

<https://creativecommons.org/publicdomain/mark/1.0/>

Access to this work was provided by the University of Maryland, Baltimore County (UMBC) ScholarWorks@UMBC digital repository on the Maryland Shared Open Access (MD-SOAR) platform.

Please provide feedback

Please support the ScholarWorks@UMBC repository by emailing scholarworks-group@umbc.edu and telling us what having access to this work means to you and why it's important to you. Thank you.

A View of the Inner Heliosphere During the May 10-11, 1999 Low Density Anomaly

Arcadi V. Usmanov

Institute of Physics, University of St.-Petersburg, St.-Petersburg 198904, Russia

Melvyn L. Goldstein, William M. Farrell

NASA/Goddard Space Flight Center, Greenbelt, MD 20771, USA

Abstract. On May 10 and 11, 1999, near-Earth spacecraft observed the solar wind density drop to below 0.1 particles cm^{-3} . Using those data, we have mapped solar wind parameters back to the Sun from 1 AU using two techniques. The first assumed constant-velocity trajectories plus corotation, while the second employed MHD-derived magnetofluid parameters. This inverse tracing creates a view of the inner heliosphere useful for identifying the source location on the Sun of the density anomaly. We compare the two methods and show that the source location of the anomaly predicted by MHD is mapped $\sim 20^\circ$ eastward of the constant-velocity result. The coronal magnetic field maps indicate that the low density event occurred as the polar coronal magnetic field began reversing. We suggest that the event was initiated by a latitudinal excursion of the low velocity heliospheric current sheet toward the helioequator. The emergence of this slow flow into the preexisting faster wind produced strong rarefaction and anomalously low densities.

1. Introduction

The near-Earth environment frequently experiences events whose origin at the Sun is unclear. In such cases, it is useful to map solar wind parameters from 1 AU back to the Sun and to compare with solar observations to try to ascertain what coronal conditions produced the disturbance at Earth. On May 10-11, 1999, ACE, Wind, IMP 8, and other spacecraft observed that the solar wind density at 1 AU dropped below 0.1 particles cm^{-3} and the Earth's bow shock moved outward to ~ 50 Earth radii [M. Desch, A. Szabo, and D. Fairfield, private communication].

Using the kinematic constant-velocity method to map structures from 1 AU back to the Sun is fairly accurate at trailing edges of high-speed streams where there is a little interaction between fast and slow flows, but can produce large errors at the leading edges of fast streams where dynamical interactions dominate. An alternative is to integrate the MHD equations in reverse, a procedure known as inverse MHD mapping [Pizzo, 1981; Usmanov, 1993; Riley *et al.*, 1999]. If the solar wind pattern observed during a solar rotation is assumed to be stationary in the corotating frame and

dissipation is negligible, then the MHD equations are hyperbolic with respect to the radial coordinate and can be integrated backward in radius [Pizzo, 1981] while consistently accounting for the flow acceleration and dynamical interactions between flow elements. Because the equations are hyperbolic only in supersonic and super-Alfvénic flows, the solution cannot be brought closer to the Sun than 0.1–0.2 AU. Strong latitudinal variations in the outer corona cannot be

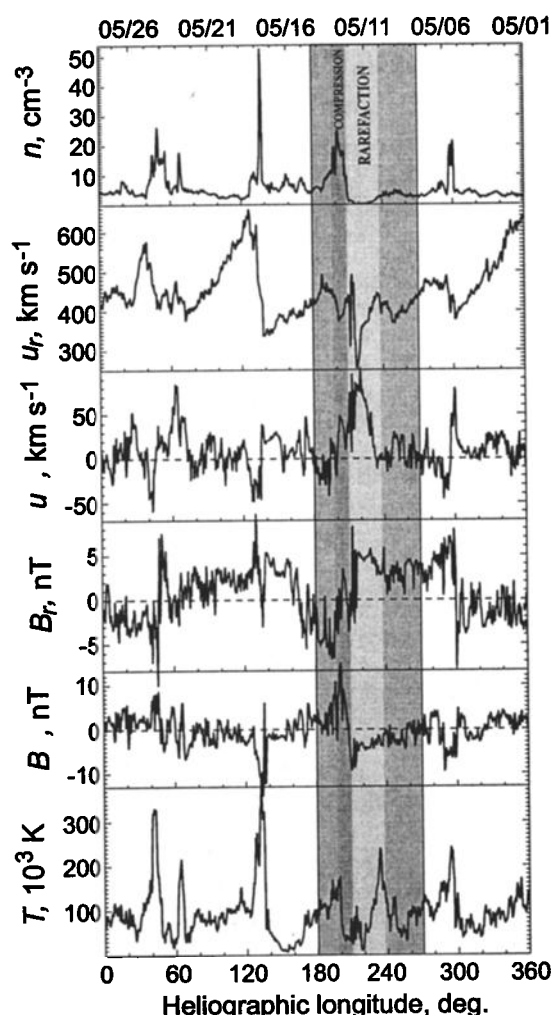


Figure 1. Hourly averages from the ACE plasma and magnetic field experiments versus heliographic ϕ for solar rotation 1949 beginning May 1, 1999. Corresponding regions in Figures 4 and 5 are shaded.

Copyright 2000 by the American Geophysical Union.

Paper number 2000GL000082.
0094-8276/00/2000GL000082\$05.00

computed because the input data at 1 AU are essentially two-dimensional.

We use the inverse MHD technique to infer conditions in the outer corona using ACE plasma and magnetic field data during solar rotation 1949. We compare the inverse MHD solution with the constant-velocity mapping and with the coronal magnetic fields as determined at the Wilcox Solar Observatory (WSO). We explore the low density event in association with the evolution of large-scale magnetic fields at the Sun and suggest a possible cause.

2. Modeling

We assume that the solar wind can be regarded as a single-fluid polytropic flow with negligible dissipation. The resulting two-dimensional, steady-state MHD equations in the equatorial plane (r, ϕ) are given in [Usmanov, 1993]. The dependent variables are the mass density ρ , radial velocity u_r , azimuthal velocity u_ϕ , radial magnetic field B_r , and thermal pressure P . In steady-state, solar wind plasma flows along the magnetic field in the corotating frame and the az-

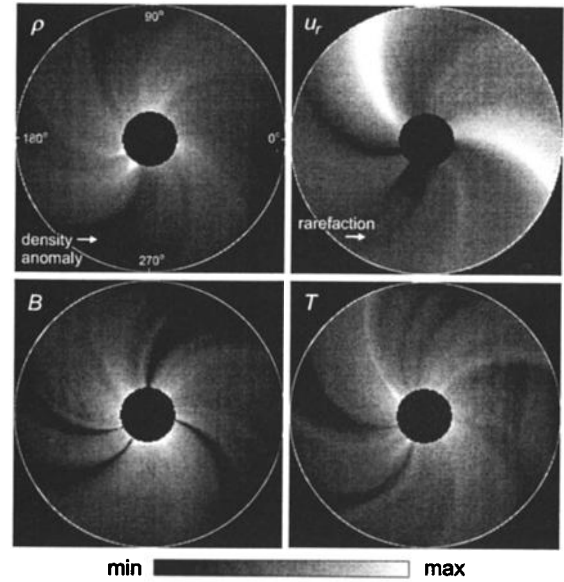


Figure 3. Gray-scale images of ρ , u_r , B , and T in the equatorial plane from the MHD inverse mapping for solar rotation 1949. The view is from the north pole of the Sun; the inner boundary is at 0.2 AU and the outer is at 1 AU.

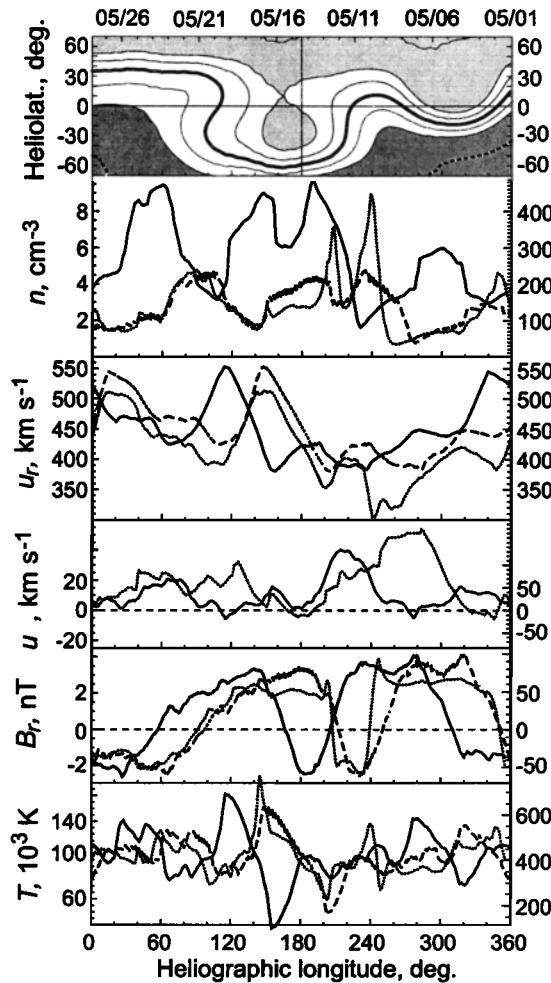


Figure 2. Solar wind and magnetic field parameters versus heliographic longitude for rotation 1949 mapped to 0.2 AU using constant-velocity with corotation (dashed lines) and MHD (dotted lines) methods (right hand scales). Initial data at 1 AU are solid lines (left hand scales). Upper panel: a contour map of the coronal field at $3.25 R_\odot$ from the WSO.

imuthal magnetic field is given by $B_\phi = v_\phi B_r / u_r$, where $v_\phi = u_\phi - \Omega r$ is the azimuthal velocity in the corotating frame and Ω is the solar sidereal rotation rate.

We use ACE observations (Figure 1) to specify initial conditions at 1 AU. We averaged these data using a 72-hour (3-day) running average to filter out most of the time dependence. The smoothed flow and magnetic field profiles (solid lines in Figure 2) are assumed to be steady and are used as input to integrate the flow and magnetic field back to 0.2 AU. The polytropic index is taken to be $\gamma = 3/2$ [Totten *et al.*, 1995] to account implicitly for non-adiabatic expansion caused by thermal conduction.

3. Results and Discussion

Figure 2 summarizes our results using both methods. To avoid double-valued profiles, the constant-velocity method was modified using a step-by-step radial integration in 1-hour intervals. The two methods differ significantly. For example, a difference of $\sim 10^\circ$ is seen in the velocity projections at the leading edges of higher-speed flows, while the trailing edges coincide fairly well. The MHD method produces smaller velocities at 0.2 AU because of the acceleration that results from the MHD solutions. The largest deviation in u_r , of up to $\sim 100 \text{ km s}^{-1}$, occurs at $\phi \sim 240\text{--}270^\circ$, close to the source longitudes of the density anomaly. Figure 2 shows that the inferred position of the density anomaly at 0.2 AU from the MHD mapping is $\sim 20^\circ$ eastward of the position obtained from the constant-velocity method. This is primarily a result of the large positive (westward) azimuthal velocity u_ϕ observed at $200\text{--}240^\circ$ which is also responsible for the difference in the position of the sector boundary close to the density anomaly. In a run using $u_\phi = 0$ (i.e., no east-west flow), the source position was almost identical

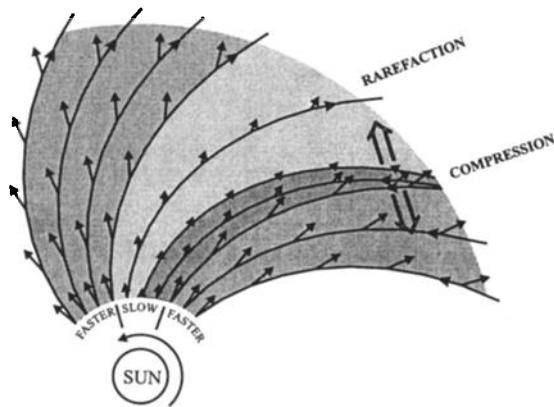


Figure 4. A schematic of the stream interaction in the equatorial plane of the inertial frame with slow wind between the faster wind regions. The view is from north of the heliospheric equator. Small arrows indicate flow vectors and the direction of the magnetic field. Large open arrows show secondary lateral motions driven by pressure gradients produced by the compression region. The shading corresponds to that in Figures 1 and 5.

to that obtained using the constant-velocity approximation. Therefore, the east-west flow is the primary source of the longitudinal shift in the source region.

The heliospheric field during rotation 1949 had a four-sector structure. A comparison of the projected profile of B_r at 0.2 AU with the WSO coronal field at $3.25 R_\odot$ (solar radii) shown at top of Figure 2 reveals reasonable agreement in the longitudes where the heliospheric current sheet crosses the helioequator. Because it takes about 0.8 days for solar wind to reach 0.2 AU, the projected curves should be shifted by an additional $\sim 10^\circ$ to the right for a better comparison with the WSO map.

Figure 3 shows flow parameters in the equatorial plane between 0.2 and 1 AU as images with a logarithmic scale for ρ , B , T and a linear scale for u_r . A spiraling four-sector structure is seen clearly in B with darker regions around sector boundaries. This four-sector structure is discernable as an increase in u_r and T inside sectors and in ρ near the sector boundaries. A wide region of low density lies close to a sector boundary. This region is followed by a compression across the sector boundary. An extensive region of low velocities overlaps the low-density region and is followed by the sector boundary (after which the velocity increases).

Figure 4 suggests an interpretation of the stream dynamics involved in the formation of the density anomaly. The figure shows a schematic of interacting streams in the ecliptic plane; slow wind is found in-between faster flows. Due to solar rotation, the plasma in the slow wind forms a rarefaction region, while the following faster flow creates a compression. This schematic suggests that rarefaction should be followed by a compression which can be confirmed from Figure 5. Material piling up at the trailing edge of the slow speed stream (where fast wind overtakes slow wind) drives non-radial flows directed away from the compression region ($u_\phi > 0$ before the compression and $u_\phi < 0$ after it), as seen in the ACE data.

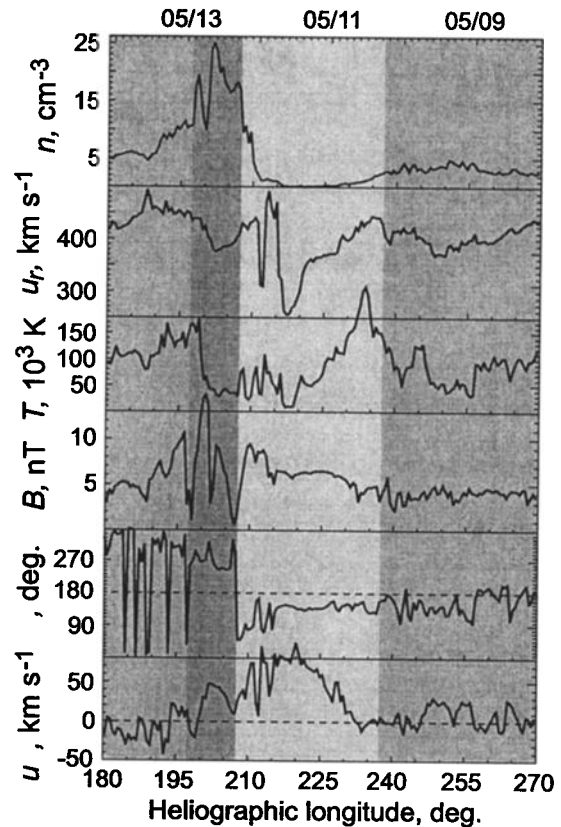


Figure 5. A plot of the hourly ACE data across the low-density event. B and the spiral angle (ϕ) of the magnetic field are shown. The shading corresponds to that in Figures 1 and 4.

The absence of a prominent depletion in the field magnitude across the low density anomaly may reflect the magnetic field distribution near the Sun and also the fact that the magnetic field is mostly radial and aligned with the flow up to large heliocentric distances. The magnetic depletion can be, therefore, much less pronounced than that in density.

Both in the schematic and in the ACE data, the slow-speed stream is located near a sector boundary where both B_r and B_ϕ change sign, the observed velocity drops to $\sim 250 \text{ km s}^{-1}$, and T is also at a minimum. Note that the

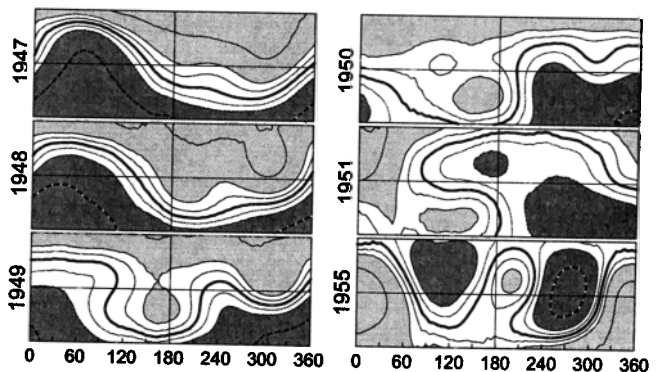


Figure 6. A sequence of the source surface field maps from the Wilcox Solar Observatory for solar rotations 1947-1951 and 1955. The neutral line is a heavy line and the regions of negative polarity are shaded more darkly.

schematic in Figure 4 is different from that in Hundhausen [1972] and Pizzo [1978], where fast flow was shown between slow streams and the time sequence of compression and rarefaction was reversed.

To find the origin of the slow velocity region, we compiled a sequence of the WSO source surface maps both before and after rotation 1949. Figure 6 shows that before rotation 1949, the coronal structure (the radial magnetic field at a source surface located at $3.25 R_{\odot}$) was approximately steady, but rapid evolution is apparent on subsequent rotations. Before rotation 1950 the radial field is positive north of the neutral (heavy) line and negative to the south, but the polarity of the Sun's polar field has reversed by rotation 1955. The transformation began with a northward excursion of the neutral line (which is usually considered to be at the base of the heliospheric current sheet where slow solar wind originates) at longitudes ~ 220 – 270° toward and across the helioequator. Not coincidentally, solar activity also increased significantly in May, 1999. We suggest that the northward excursion of the heliospheric current sheet is associated with the source of slow wind.

Because the schematic of the low-velocity corotating structure (Figure 4) is constructed assuming steady-state, we cannot exclude the possibility that the observations at least partially result from unidentified transients in the corona. If a transient is associated with this density anomaly, then the inverse MHD mapping should still be useful in localizing where it occurred. Either the source of the slow stream formed during rotation 1949 and corotated past the Earth, or the Earth was at the right time and place to encounter the transient formation of the low-speed corotating structure.

Our interpretation suggests that at the beginning of any solar activity cycle the initial deformation of the heliospheric current sheet as the polar fields reverse will produce density anomalies. Studies of previous solar cycles indicate that such anomalies are indeed associated with the rising phase of solar activity [Ogilvie *et al.*, 2000].

4. Conclusions

Our main points may be summarized as follows:

1. The inverse MHD mapping is a useful tool for determining which coronal structures produce the solar wind observed at 1 AU. Using the MHD equations to project backward takes into account dynamic interactions in the fluid as well as the acceleration of the flow. The method is restricted to steady state super-sonic/super-Alfvénic flows.
2. The solar wind sector structure deduced from inverse mapping agrees with that inferred from WSO data. Constant-

speed mapping leads to large errors, especially at the leading edges of high speed stream and near density anomalies. The source of the density anomaly mapped by MHD is located $\sim 20^{\circ}$ eastward of the constant-velocity projection.

3. WSO coronal maps show that the density anomaly event took place at the beginning of a period of global change in the coronal magnetic field that preceded the reversal of the solar polar field. The inverse mapping technique cannot be used for later time periods because increasing solar activity invalidates the steady state assumption.

4. We suggest that the density anomaly was produced by slow flow emerging into preexisting fast flow as the heliospheric current sheet deformed and extended northward across the helioequator during solar rotation 1949. This mechanism should be applicable to other depletion events, especially at the beginning of new solar activity cycles.

Acknowledgments. We are grateful to the SWEPAM team (D. J. McComas, P.I.) and the MAG team (N. F. Ness, P.I.) for providing ACE plasma and magnetic field data via the ACE Science Center web site. Wilcox Solar Observatory data was obtained from site <http://quake.stanford.edu/~wso>, courtesy of J. T. Hoeksema.

References

- Hundhausen, A. J., *Coronal Expansion and Solar Wind*, 329 pp., Springer-Verlag, New York, 1972.
- Ogilvie, K.W., R. Fitzenreiter, and M. Desch, Electrons in the low density solar wind, *J. Geophys. Res.*, submitted, 2000.
- Pizzo, V. J., A three-dimensional model of corotating streams in the solar wind: 1. Theoretical foundations, *J. Geophys. Res.*, **83**, 5563–5572, 1978.
- Pizzo, V. J., On the application of numerical models to the inverse mapping of solar wind flow structures, *J. Geophys. Res.*, **86**, 6685–6690, 1981.
- Riley, P., et al., Relationship between Ulysses plasma observations and solar observations during the Whole Sun Month campaign, *J. Geophys. Res.*, **104**, 9871–9879, 1999.
- Totten, T. L., J. W. Freeman, and S. Arya, An empirical determination of the polytropic index for the free-streaming solar wind using Helios 1 data, *J. Geophys. Res.*, **100**, 13–17, 1995.
- Usmanov, A. V., MHD projection toward the Sun of a solar wind structure observed at the Earth's orbit, *Geomag. Aeronom.*, **33**, 394–395, 1993.
- W. M. Farrell, M. L. Goldstein, NASA/Goddard Space Flight Center, Greenbelt, MD 20771, USA. (e-mail: william.farrell@gsfc.nasa.gov; melvyn.goldstein@gsfc.nasa.gov)
- A. V. Usmanov, Institute of Physics, University of St.-Petersburg, St.-Petersburg 198904, Russia. (e-mail: usmanov@snoopy.phys.spbu.ru)

(Received April 11, 2000; revised July 10, 2000; accepted July 20, 2000.)